

Traceable Measurement of Power Losses in HVDC Converter Valves

V. Ermel², E. Mohns¹, J. Meisner¹, O. Binder², W. Lucas^{1*}, M. Kahmann¹, M. Kurrat²

¹ Physikalisch-Technische Bundesanstalt, Germany, ² Technische Universität Braunschweig

*Email: <Wolfgang.Lucas@ptb.de>

Abstract: A European research programme for the metrology of HVDC energy transmission has started. This includes work packages for the loss evaluation of HVDC converters, drawing up concepts and the construction of HVDC dividers, power quality and dc metering. This paper describes the progress and first results for loss evaluation. To cover their needs a cooperation between the Physikalisch-Technische Bundesanstalt and the Technische Universität Braunschweig has been established.

1 INTRODUCTION

The expanding market for renewable energy demands the implementation of HVDC transmission lines to provide energy transportation from the remote production sources. The additional feature of a dc transmission system to mitigate power fluctuations ensures that dc technology plays an important role in modern power grids. The growing role of dc transmission in a globalised world requires the precise assessment of the transported energy. The accurate evaluation of power losses at converter stations as well as a measurement of the power flow over dc lines provides necessary conditions for international trade. A European research programme [1] is intended to provide the metrological support for the needs of HVDC energy transmission.

2 POWER STANDARD FOR INTEGRAL POWER EFFICIENCY OF CONVERTERS

One planned outcome of this programme is to establish standards for determining the power losses of a converter by measuring its integral power efficiency. Due to the required high analogue bandwidth when assessing the power efficiency of converters, so-called power analysers with bandwidths of several hundreds of kHz and suitable wideband ac and dc voltage and current transducers are widely used. To avoid the simultaneous generation of high ac and dc voltage and current levels to emulate the typical amount of power and energy of a converter, the calibrations of the relevant components will be performed separately. To offer traceable calibrations of power analysers with measurement uncertainties in the order of 0.03 %, a precise wideband power standard with inputs for ac and dc signals has to be developed. Furthermore, the capabilities of the existing measurement systems for calibrating ac voltage- and current transformers, of the dc voltage

divider and the current sensors, have to be extended [2-4] for appropriate wideband operation.

2.1 Emulation of converter signals

In a first step, the generation of distorted signals for emulating typical ac and dc signals of different converter topologies is investigated. According to fig. 2a, a digital IIR low pass pre-filter processes the idealised converter waveforms to emulate the limited bandwidth of a real converter. To avoid the Gibbs phenomenon when processing non-bandwidth-limited signals (e.g. rectangular pieces of a signal), the digital filter routine is modified using bilinear transform (Tustin's method) in the frequency domain.

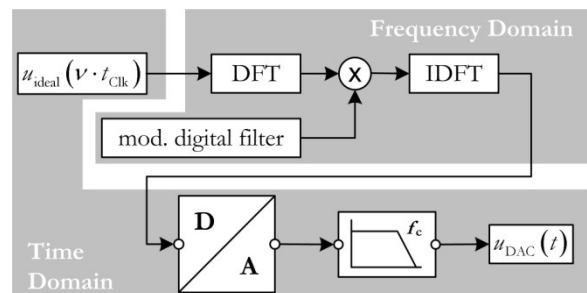


Figure 2a: Scheme of the generation of converter signals

An arbitrary waveform generator (AWG) with a resolution of 16 bits is programmed with these pre-filtered waveforms. Subsequently, the generated waveforms are filtered analogue to eliminate any high frequency artifacts from the digital signal processing. To show the effectiveness of the combination of digital pre-filtering and analogue post-filtering, an ideal 3-level square wave signal with a fundamental frequency of 50 Hz is generated with $n = 10,000$ steps. The digital pre-filter (6th order Bessel filter) is set to a cutoff frequency of 50 kHz. The analogue low-pass filter (2nd order Butterworth filter) is adjusted for a cutoff frequency of 60 kHz. A 24-bit digitiser samples the

waveforms with a sampling frequency of 2 MHz. The three waveforms (without any filtering → “DAC direct”; digital filter only → “DAC + DF”; digital and analogue filtering → “DAC + DF + AF”) and the associated Fourier spectra are shown in fig. 2b.

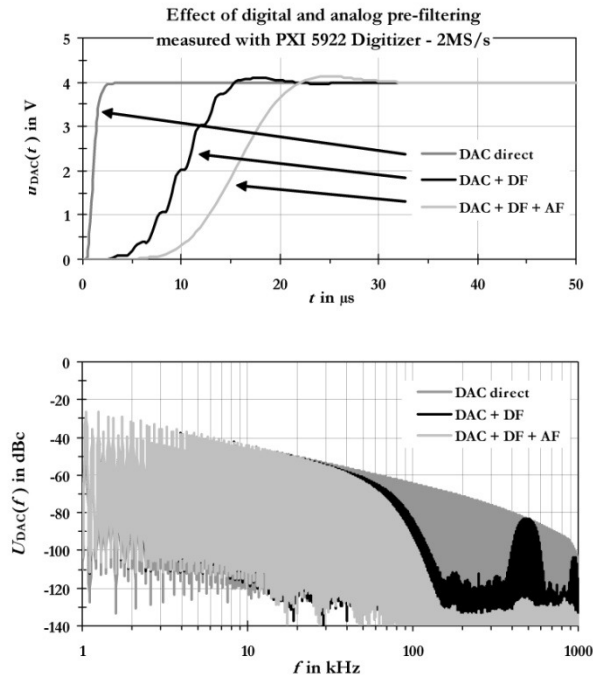


Figure 2b: Generation of a 3-level rectangular waveform. The rising edges of the waveforms are highlighted (upper diagram). The lower diagram shows the Fourier spectra of the waveforms.

The smoothed rising edges clearly show the effect of the digital and analogue pre-filtering. The Fourier spectra show that the combination of the two filters leads to signals with a strictly controlled bandwidth and noise levels well below -120 dBc. Such signal purity is necessary for the future calibration setup, where these converter waveforms are fed to wideband voltage and transconductance amplifiers to generate the test signals for the power analyser (device under test) and the reference measurement system.

3 ENERGY LOSSES OF IGBTs

3.1 Energy distribution in the frequency domain

Power converters exhibit a broad frequency spectrum up to MHz harmonics generated through switching of the semiconductors in valves. Energy distribution in the frequency domain depends on the converter topology and its operation mode. The acquirement of the converter frequency spectrum appoints a sampling rate of the digital measurement system to deliver the data set of a predefined uncertainty.

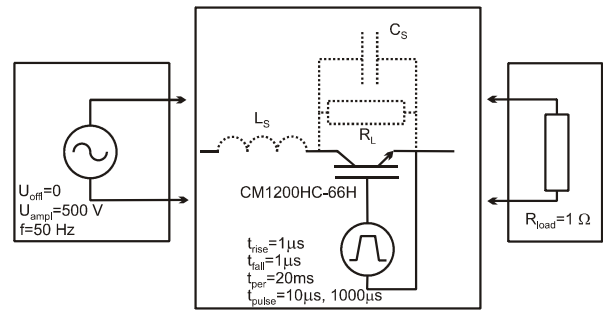


Figure 3a: IGBT switch in resistive operation mode

The frequency spectrum of an IGBT circuit is investigated with the model presented in fig. 3a. The model includes the ORCAD (PSPICE) voltage source applied to the resistive load through the IGBT switch. It is modelled by stray inductance L_s of 200 nH, stray capacitance C_s of 10 pF and leakage resistance R_L of 1 MOhm. The IGBT gate is controlled by a pulse source delivering 10 μ s or 1000 μ s pulses with a rise and fall time of 1 μ s. The time interval between the pulses is 20 ms. Transient parameters of the IGBT and of a free-wheeling diode (FWD) are defined from the data set of the high power switch MITSUBISHI CM1200HC-66H. The IGBT and the FWD are modelled as a set of the following behavioural equations:

$$\begin{aligned}
 \text{IGBT: } I_{fall} &= f(t) & \text{FWD: } I_{fwd} &= f(U_{fwd}) \\
 I_c &= f(U_g) & C_{rev} &= f(U_{rev}) \\
 U_{ce} &= f(I_c) & I_{rev} &= f(U_{rev}) \\
 U_{ge} &= f(Q_g) & U_{br} &= f(I_{br}) \\
 & & I_{fwd} &= f(t)
 \end{aligned}$$

where I_{fall} - current fall, I_c - collector current, U_{ce} - collector-emitter voltage, U_{ge} - gate voltage (all of IGBT), I_{fwd} - forward current, C_{rev} - reverse capacitance, I_{rev} - reverse current, U_{br} - breakdown voltage (all of FWD).

The simulated voltage curves and transients are analysed with the MATLAB software. In the following the Fourier spectrum is calculated (see fig. 3b) to be converted to its square value defining the power density spectrum (PDS).

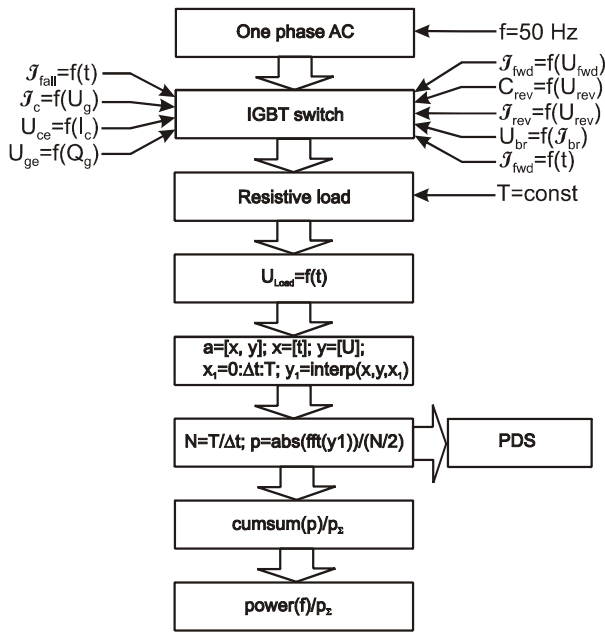


Figure 3b: Computation of power density spectrum and cumulative sum

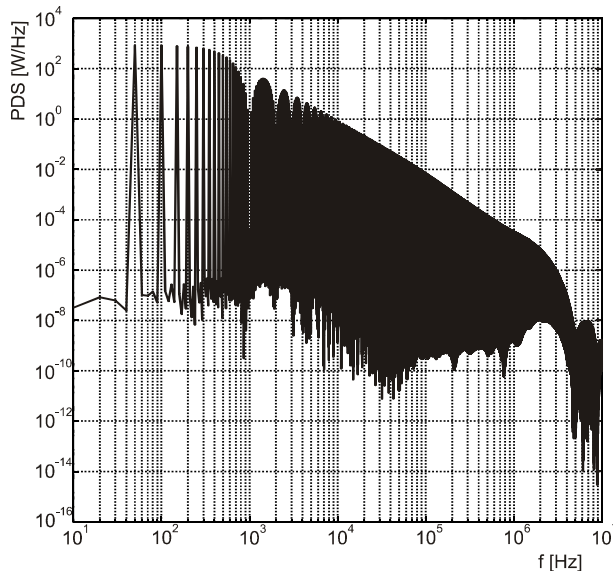


Figure 3c: Power density spectrum of 1 ms modulation voltage pulse

Fig. 3c shows the PDS of a 1 ms pulse simulated in the frame of the circuit model shown in fig 3a. It is presented in logarithmic scale to show the whole range up to MHz harmonics. The fundamental frequency, its low harmonics and modulation components dominate the spectrum.

Furthermore, the cumulative sum of the PDS harmonics $\sum_{i=1}^{i=k} p_i$ is calculated and normalised to

the sum of harmonics $\sum_{i=1}^{i=f \max} p_i$ over the whole spectrum.

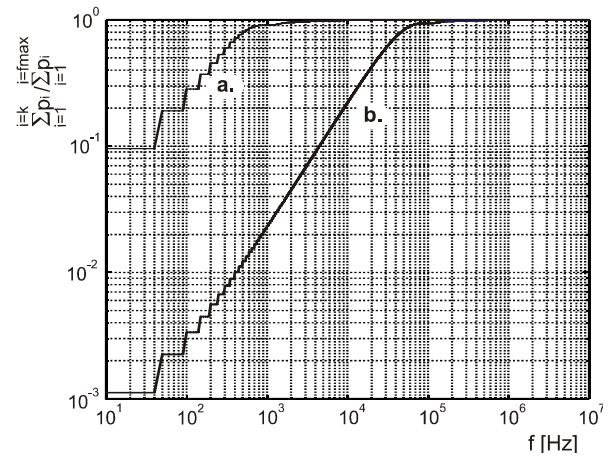


Figure 3d: Normalised cumulative sum of PDS of 1000 μ s (a.) and 10 μ s pulses (b.)

Fig. 3d shows the normalised cumulative sum of the power density spectrum of 1000 μ s (a.) and 10 μ s (b.) modulation pulses. The curves exhibit a drastic growth of power components in the low frequency range. An increase of the pulse time shifts the power distribution to lower frequencies. From the normalised cumulative sum the required bandwidth of the measurement system can be extracted to reach a predefined uncertainty level of the dissipated energy. This is shown in table 3a for the circuit modulation run of 1000 μ s.

Table 3a: Frequency range of PDS

Normalised sum of PDS harmonics	0.9	0.99	0.999
Frequency [kHz]	1.5	9	65

3.2 Energy loss in inductive IGBT circuit

The test circuit is constructed assuming inductive operation mode (see fig. 3e). It includes a high voltage dc power unit, consisting of three-phase adjustable transformers T_1 and T_2 . A six pulse rectifier D_1 charges the capacitor bank C_1 . IGBT₁ and IGBT₂ are connected in series. The experimental investigations are carried out with a large capacitor bank delivering enough energy for a pulse sequence. The bank comprises an array of high voltage capacitors connected together over the low-inductance plate transmission line. The storage system consists of 60 μ F capacitors with a rated voltage of 2.5 kV. The total capacitance of the storage bank amounts to 18 mF.

The large low-resistance coil L_1 is connected in parallel to the IGBT₁ and determines the current transient during the switching of IGBT₂. The coil inductance amounts to 4.4 mH at its resistance of 0.6 Ohm. To calculate the energy losses, a voltage divider VD and resistor R_S are used to measure the voltage and current signals with a digital recorder.

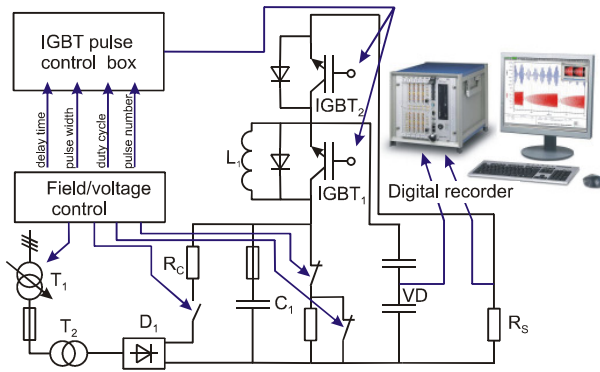


Figure 3e: IGBT circuit in inductive operation mode

The voltage and current transients are acquired with a calibrated digital transient recorder. Three optically isolated satellites are used to acquire the gate control pulses of the IGBTs, the collector voltage of the IGBT₂ and the pulse current.

The time varying power losses $p_v(t) = u_{ce}(t) \cdot i_c(t)$ and the energy losses E_v of the IGBT₂ are calculated according to

$$E_v = \Delta t \cdot \sum_{i=1}^N p_v(i).$$

The energy E_S dissipated in R_S is calculated from $p_S(t) = u_{RS}(t) \cdot i_c(t)$ and

$$E_S = \Delta t \cdot \sum_{i=1}^N p_S(i).$$

The investigations are carried out by pulse time settings of 1 ms, 1.2 ms and 1.6 ms. The charge voltages are 100 V, 120 V and 140 V. The switching transients are recorded with a sampling rate of 100 MS/s. The sampling rate is adjusted to 1 MS/s during measurement of the conductive phase of IGBT.

The calculated energy losses are presented in fig. 3f for the pulse time setting of 1 ms. The curves exhibit a quadratic behaviour due to rising energising of the large coil. The switch-off of IGBT causes further energy loss seen as a quick growth of the curve at the end of commutation.

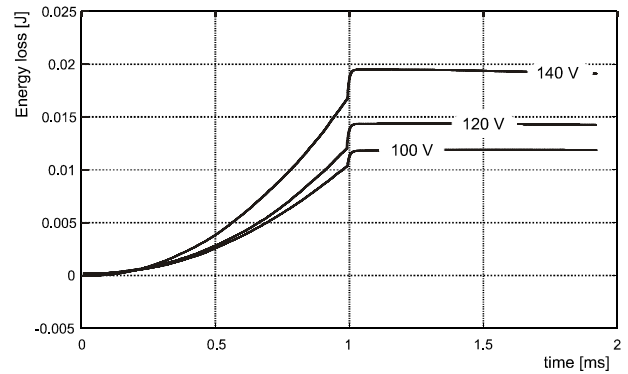


Figure 3f: IGBT energy loss

A summary of the energy loss is presented in table 3b. An increase of the pulse time causes nonlinear growth of conductive losses; likewise an increase of the charge voltage drastically causes growth in the conductive state. Compared to a continuous inductive operation mode of the converter valve, the switching in the pulsed inductive operation mode delivers a quasi-linear increase of the commutated current followed by a nonlinear increase of the conductive losses. Switch-off losses show some linear growth with an increase of the pulse time. Increasing the charge voltage leads to the nonlinear growth of the energy loss due to the effect of both the applied voltage and the commutated current.

Table 3b: Energy loss and load energy

Pulse time [ms]	Charge voltage [V]		
	100	120	140
<i>E_c</i> : Conductive loss [mJ]			
1	10.2	11.6	16.5
1.2	14.9	18.6	21.6
1.6	22.5	32.6	44.4
<i>E_{off.}</i> : Switch-off loss [mJ]			
1	0.64	1.02	1.45
1.2	0.8	1.25	1.75
1.6	1	1.8	2.2
<i>E_S</i> : Resistive load energy [mJ]			
1	156	239	314
1.2	284	440	571
1.6	614	941	1228

Table 3c shows the loss-to-load ratio in the range of parameters of investigation. It is apparent that an increase of the commutation time and an increase of the applied voltage improve the circuit efficiency.

Table 1c: Ratio of the loss-to-load energy

Pulse time [ms]	Charge voltage [V]		
	100	120	140
1	0.069	0.053	0.057
1.2	0.055	0.045	0.041
1.6	0.038	0.037	0.038

4 CALIBRATION OF A DIGITAL RECORDER SYSTEM

The measuring system Saturn from AMOtronic is a 4-channel digital recorder system. Each of the four measuring heads is isolated and has an analogue bandwidth of 50 MHz. The measuring heads (satellites) include analogue-to-digital converters with 14 bits at a maximum sampling rate of 100 MS/s. The recorder and the measuring heads are connected via optical fibres. To control the system and to evaluate the measuring data, the recorder consists of an integrated personal computer with the measuring software "Saturn II". [5]

The calibration of this transient recorder system included four different calibration processes: calibration with dc voltages, calibration with ac voltages at frequencies up to 1 MHz, calibration with impulse voltages and calibration with step voltages.

4.1 Calibration with dc voltages

The calibration circuit for digital recorders for dc measurements is shown in fig. 4a. The digital recorder under test is connected parallel to the PTB standard instrument. A dc calibrator (Fluke 5720A) creates the stable dc voltage which is measured by all satellites and the reference measuring system simultaneously. A low pass filter smooths all possible radio frequency disturbances. The measured values of both devices are evaluated in Excel. The ranges $\pm 5V$ and $\pm 10V$ were calibrated by measuring the dc voltages with steps of 5 % of the maximum amplitude level. The error of the system is evaluated with regard to the mean value, the standard deviation of the mean value, the offset and the expanded uncertainty.

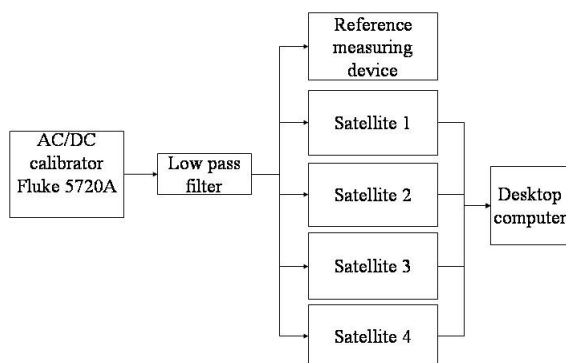


Figure 4a: Setup for dc voltage calibration

4.2 Calibration with ac voltages

The calibration circuit for digital recorders for ac measurements is shown in fig. 4b. The digital recorder to be calibrated is connected to an ac calibrator directly. The applied voltage of the device under test is recorded and analysed. The measured values are evaluated in Excel. The

ranges $\pm 5V$ and $\pm 10V$ were calibrated at least at nine points at the frequencies 100 Hz, 500 Hz, 1 kHz, 5 kHz, 10 kHz, 50 kHz, 100 kHz, 500 kHz and 1 MHz. In this case the test unit was directly connected to the ac calibrator without using cables. The ac calibrator serves as the reference for this measurement. The error of the test sample is determined with regard to the mean value, the standard deviation of the mean value, the offset and the expanded uncertainty.

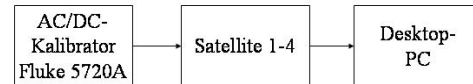


Figure 4b: Setup for ac calibration

4.3 Impulse and step-voltage calibration

The calibration of the digital recorder is made by comparing the measured values with those of the PTB standard measurement system for impulse voltage according to IEC 61083.

The basic structure of the calibration circuit for the digital recorder is shown in fig. 4c. The measuring system consists of a high voltage probe (ratio 1000:1) and the transient recorder system. The probe is connected to an impulse generator for standard pulses. Both the measurement system and the reference measuring system record and analyse the pulses. The measured values of the reference digital recorder are evaluated by the PTB software named STOSS.

The pulses generated are usually double-exponential lightning impulse voltages, 0.84/60, and switching impulse voltages, 20/4000, with peak values up to 1600 V for measurements with the probe and up to 8 V for measurements without the probe.

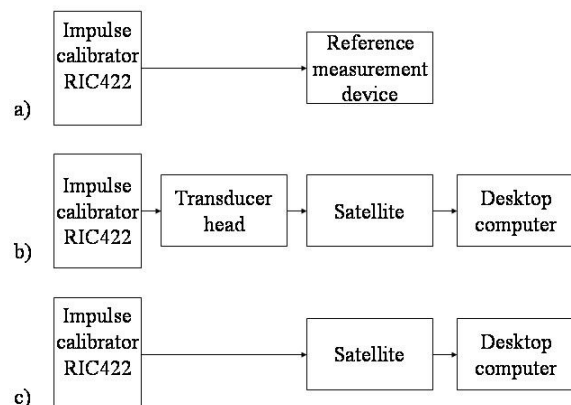


Figure 4c: Setup for impulse voltage calibration

- Reference measurement setup
- Measurement setup for 1600 V
- Measurement setup for 8 V

The measurement setup for step voltage is the same as shown in fig. 4c. The negative step voltages (step from positive voltage value to zero) were created by a mercury relay, which replaces the impulse calibrator in fig. 4c. Two different voltage values of 8 V and 200 V have been used to calibrate the measuring system with and without a high voltage probe. The errors for the peak value U , the rise time T_1 and the time to half-value T_2 have been determined. The calibration of time intervals has been done by comparing the rise time and the time to half-value of the standard measuring system and the device under test.

4.4 Calibration results

Table 4a shows the results of the described calibration of the transient recorder system. In the case of switching and lightning high impulse voltages, there is no facility to measure more precisely than 1 % at time parameters and 0.4 % at peak values. The results in dc and ac voltages as well as step voltages are less than 0.3 %.

Table 4a: Calibration results

	Performance	Expanded uncertainty
d.c.	Steps of 5% of the ranges ± 5 V and ± 10 V	modulation 30% – 100% \rightarrow $<0,07\%$ modulation 5% - 30% \rightarrow $<0,5\%$
a.c.	f = 100 Hz to 1 MHz at the ranges ± 5 V and ± 10 V	≤ 100 kHz \rightarrow $<0,07\%$ 100 kHz – 1 MHz \rightarrow $<0,3\%$
Step voltages	Step voltages with Hg-Relays 9 V and 200 V (IEC 61083-1)	$<0,3\%$
Impulse voltages	Lightning impulse (LI 0,84/60) and switching impulse (SI 20/4000) (IEC 61083-1)	Peak values: 0,4% Time parameters: 1 %

5 CONCLUSION

To set up a power standard for the integral power efficiency of converters, the emulation of converter waveforms using a 16 bit digital-to-analogue converter was investigated. A strictly controlled bandwidth and noise levels well below -120 dBc are reached using digital and analogue filtering.

To evaluate power losses on high power IGBTs, a test setup for measuring switching and conductive losses is shown. It is capable of generating voltages up to about 2 kV. A control circuit allows variable switching times of the IGBT under test.

To verify the results of the measuring system, the transient recorder used has been calibrated at PTB. The calibration is performed at dc and ac voltages as well as step and impulse voltages.

The results of this work establish the basis for further advancements for metrology of HVDC energy transmission.

6 ACKNOWLEDGMENT

The research leading to these results has received funding from the European Union on the basis of Decision No 912/2009/EC.

7 REFERENCES

- [1] Publishable JRP Summary for Project ENG07 (HVDC): "Metrology for High Voltage Direct Current", <http://www.euramet.org>
- [2] L. Zhang: "Aufbau und Untersuchung eines Spannungsteilers für Hochspannungsimpulse bis 1600 V", Diplomarbeit Fachhochschule Braunschweig/Wolfenbüttel, June 2009
- [3] E. Mohns, J. Meisner, B. Altinsoy, G. Roeissle, M. Schmidt: "Messplatz für gleichstromfähige Stromwandler", Seminar Messwandler, Technische Akademie Esslingen, 11/2010
- [4] J. Meisner, M. Schmidt, W. Lucas, E. Mohns: "Generation and Measurement of AC Ripple at High Direct Voltage", ISH 2011
- [5] J. Meisner: "Auslegung und Auswahl einer Messeinrichtung zur Erfassung der Schaltverluste von IGBT's in HGÜ-Umrichterstationen unter besonderer Berücksichtigung der Messunsicherheit", Diplomarbeit Technische Universität Braunschweig and PTB, 04/2010